analytical chemistry

Article

Cite This: Anal. Chem. 2019, 91, 10849−10855

pubs.acs.org/ac

Quantitative SO_2 Detection in Combustion Environments Using Broad Band Ultraviolet Absorption and Laser-Induced Fluorescence

Wubin Weng, Marcus Aldén, and Zhongshan Li*

Division of Combustion Physics, Lund University, P.O. Box 118, Lund SE-221 00, Sweden

ABSTRACT: Spectrally resolved ultraviolet (UV) absorption cross sections of SO_2 in combustion environments at temperatures from 1120 to 1950 K were measured for the first time in well-controlled conditions through applying broad band UV absorption spectroscopy in specially designed one-dimensional laminar flat flames. The temperature was observed to have a significant effect on the absorption cross-section profiles at wavelength shorter than 260 nm, while at the longer wavelength side, the absorption cross-section profiles have much less dependence on temperature. The absorption cross section at 277.8 nm with a value of 0.68×10^{-18} cm^2/molecule was suggested for the evaluation of the SO_2 concentration because of the weak dependence on temperature. To make spatially resolved measurements, laser-induced fluorescence (LIF) of SO_2 excited by a 266 nm laser was investigated. Spectrally resolved LIF signal was analyzed at different temperatures. The LIF signal showed strong dependence on temperature, which can potentially be used for temperature measurements. At elevated temperatures, spatially resolved LIF SO_2 detection up to a few ppm sensitivity was achieved. Combining UV broad band absorption spectroscopy and LIF, highly sensitive and spatially resolved quantitative measurements of SO_2 in the combustion environment can be achieved.

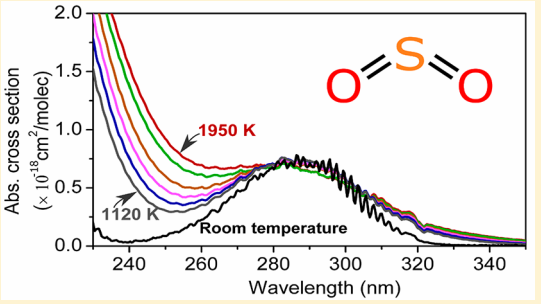

Sulfur chemistry plays a key role in the combustion/gasification of many solid fuels.[1,2] In the chemical reaction loops, one of the dominate sulfur compounds is sulfur dioxide (SO_2), which affects thermal conversion processes of fuels by interacting with the O/H radicals.[3] SO_2 released from furnaces and combustors is also an important contribution to the air pollution.[4] Hence, it is essential to perform quantitative SO_2 detection in combustion environments for comprehensive understandings of the reaction processes. Optical diagnostics, including broad band ultraviolet (UV) absorption spectroscopy,[5−10] laser-induced fluorescence (LIF),[11] and tunable diode laser absorption spectroscopy (TDLAS),[12] have been widely employed for the measurement of SO_2, which permit real-time and highly sensitive monitoring.

UV absorption spectroscopy is a reliable and low-cost method providing quantitative measurements of SO_2. For reliable quantitative measurements, accurate UV absorption cross sections of SO_2 are essential, which have been the research focus of many studies,[5,7] and it was found that the absorption cross sections could be affected strongly by temperature, as investigated by Vandaele et al.,[5] Vattulainen et al.,[6] Grosch et al.,[7] Mellqvist and Rosén,[8] and Hippler et al.[13] However, except for Hippler et al.,[13] who have investigated the UV absorption spectrum of SO_2 over the temperature range 800−4000 K in shock-wave experiments, most UV absorption cross sections are available only for the temperature up to 1073 K,[6] which cannot satisfy the measurements in normal combustion/gasification environments with a temperature varying from 1000 to 2000 K. Hence, one focus of the present work was on obtaining accurate UV absorption cross sections of SO_2 in combustion environments at 1120−1950 K.

UV absorption spectroscopy is limited to its line-of-sight nature and cannot provide spatially resolved information. To achieve spatially resolved SO_2 measurement with high sensitivity, LIF can be adopted using lasers at different wavelengths (~170 to ~338 nm) in the UV absorption region.[14] To avoid low fluorescence quantum yield due to predissociation, a wavelength threshold located near 200 nm was suggested.[15] Rollins et al.[14] developed a LIF instrument using the fifth harmonic of a tunable diode laser with a wavelength of 216.9 nm for measurements of SO_2 in the upper troposphere and lower stratosphere with a precision of 2 ppt. Matsumi et al.[11] used the second harmonics of an optical parametric oscillator pumped by the third harmonic of a Nd:YAG laser at around 220 nm to achieve SO_2 measurements with a sensitivity of 5 ppt. Fotakis et al.[16] have used the KrF laser (248 nm) to have a two-photon UV excitation of SO_2 for the laser-induced fluorescence from SO. Zhang et al.[17] investigated the fluorescence emission of SO_2 at room temperature with an excitation source of the fourth harmonic of a Nd:YAG laser at 266 nm. Sick[18] and Honza et al.[19] also measured the fluorescence signal of SO_2 with the excitation of 266 nm laser, and they found that the signal had a strong dependence on the temperature. Much stronger emission could be obtained in an atmosphere at higher temperature. This characteristic might provide benefits to the study of

Received: May 31, 2019
Accepted: July 31, 2019
Published: July 31, 2019

DOI: 10.1021/acs.analchem.9b02505
Anal. Chem. 2019, 91, 10849−10855

Table 1. Flame Conditions

	gas flow rate (sL/min)						
	jet flow			coflow			
flame case	CH_4	air	O_2	N_2	air	global equivalence ratio, ϕ	gas product temperature, T (K)
T1O2	2.95	19.20	2.09	6.84	7.09	0.78	1950
T2O2	2.66	17.34	1.89	10.84	7.74	0.74	1750
T3O2	2.48	12.24	2.58	18.97	8.90	0.70	1550
T4O2	2.28	11.89	2.26	22.69	9.82	0.67	1390
T5O2	2.09	10.90	2.07	26.51	10.66	0.63	1260
T6O2	1.71	8.91	1.68	26.92	10.25	0.60	1120
T2O1	2.66	17.34	1.89	6.95	11.61	0.67	1770
T2O3	2.66	17.34	1.89	14.21	4.37	0.83	1760
T2O4	2.66	17.34	1.89	18.60	0	0.96	1790
T2O5	3.05	17.11	1.86	13.95	0	1.12	1840
T2O6	3.14	15.53	1.91	12.09	0	1.22	1890
T2O7	3.23	14.16	1.93	9.30	0	1.32	1750
T5O1	2.09	10.90	2.07	25.11	12.05	0.61	1260
T5O4	2.09	10.90	2.07	37.20	0	0.96	1260
T5O7	2.48	8.47	1.99	22.32	0	1.31	1340
T0	0.00	27.90	0.00	18.60	12.05		296

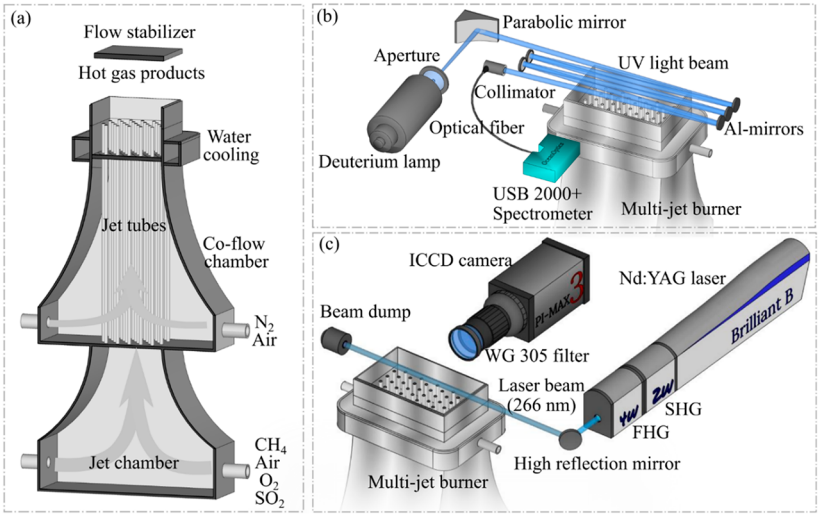

Figure 1. Schematic of (a) the multijet burner and the optical diagnostic setup including (b) the broad band UV absorption spectroscopy system and (c) the 266 nm laser-induced fluorescence system.

combustion environments with a high temperature. However, detailed information on the relationship between fluorescence emission and the temperature is still lacking. In our work, this correlation was obtained, and was used in the evaluation of the SO_2 concentration.

At the end, these two techniques, that is, broad band UV absorption spectroscopy and LIF, were compared for their application in SO_2 measurement in a combustion atmosphere, and the combination of these two techniques were discussed, aiming at the spatially resolved quantitative measurement of SO_2.

EXPERIMENTAL SECTION

Burner and Flame Conditions. A laminar flame multijet burner was used to provide different homogeneous hot gas environments with varying temperatures and fuel/air equivalence ratios. The flame cases adopted in the present study are summarized in Table 1. The temperature of the hot flue gas was varied from 1120 to 1950 K, which were measured through the two-line atomic fluorescence thermometry with indium atoms, as reported by Borggren et al.[20] The global equivalence ratio of the introduced gas was varied from 0.63 to 1.32, to produce different oxidative or reductive hot gas environments. The details of the burner were introduced by Weng et al.[21] As shown in Figure 1a, it consisted of two chambers, that is, jet chamber and coflow chamber. The jet chamber was used to mix the premixed gases, CH_4/air/O_2, and introduce it evenly to the 181 jet tubes to form laminar flames for producing the hot flue gases. The coflow chamber was used to provide the coflows, N_2/air, which surrounded the premixed jet flames evenly. In the present work, SO_2 (1% of SO_2 in N_2) was introduced into the hot flue gas through the jet flows as shown in Figure 1a. The measurements were conducted at 5 mm above the outlet of the burner. The outlet had a size of 85 × 47 mm. All flows were controlled by mass flow controllers with an accuracy of 0.5% × reading + 0.1% × full scale (Bronkhorst).

DOI: 10.1021/acs.analchem.9b02505
Anal. Chem. 2019, 91, 10849−10855

UV Absorption Spectroscopy. The schematic of the broad band UV absorption spectroscopy system is shown in Figure 1b. The UV light from a deuterium lamp was collimated by a parabolic mirror with a reflected focal length of 152 mm to form a light beam with a diameter of around 1 cm. The light beam passed through the hot flue gas with its center 5 mm above the burner using five UV-enhanced aluminum mirrors. The light was collected by a collimator and analyzed by a spectrometer (USB 2000+, Ocean Optics) with a spectral resolution of about 0.4 nm. The accumulation time of the spectrometer was set to 1 s. The total path length was estimated on the basis of the distribution of the LIF signal of SO_2 excited by a 266 nm laser (see Figure 2b), which will be illustrated in the following section.

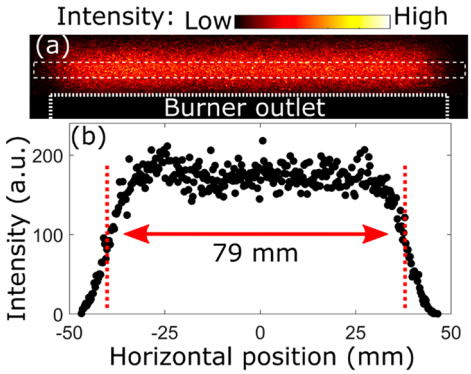

Figure 2. Typical image (a) and the horizontal distribution (b) of the laser-induced fluorescence signal of SO_2 excited by the 266 nm laser beam passing above the burner.

Laser-Induced Fluorescence System. As shown in Figure 1c, a 266 nm laser with a pulse energy of about 28 mJ/pulse was provided by the fourth harmonic of a Nd:YAG laser. The collimated laser beam with a diameter of around 8 mm was guided through the hot flue gas zone with its beam center around 5 mm above the outlet of the burner. The 266 nm laser excited SO_2 to produce broad band UV fluorescence, and the fluorescence was collected by an ICCD camera (Princeton Instruments, Model PI-MAX3, 1024 × 1024 pixels) through a long pass filter, WG305, which was used to block the laser scattering signal. The camera had an exposure time of 50 ns. The typical image of the LIF signal of SO_2 is presented in Figure 2a. The horizontal distribution of the signal in the region marked by the dash line box is presented in Figure 2b, and it was used to calculate the total path length of the UV light in the hot flue gas as shown in Figure 1b. The decrease of the signal at the edge of the flue gas was mainly caused by the lower local temperature and SO_2 concentration with the entrainment of ambient air. Moreover, a spectrometer (Andor, Model Shamrock 750, f/9.7) with a grating of 300 lines/mm was adopted for the analysis of the spectrum of the fluorescence from 190 to 350 nm with a spectral resolution of around 0.055 nm.

RESULTS AND DISCUSSION

UV Absorption Spectroscopy of SO_2. To apply UV absorption spectroscopy for quantitative measurements of SO_2 in high-temperature environments, the UV absorption cross section, $\sigma(\lambda)$, of SO_2 at different wavelength λ and temperature is needed. In the present study, the absorption cross section at the temperature varying from 1120 to 1950 K is obtained based on the Beer-Lambert law:

$$\sigma(\lambda) = A(\lambda)/(NL) = -\ln\left(\frac{I_s(\lambda)}{I_0(\lambda)}\right)/(NL) \quad (1)$$

where A is the absorbance, which is derived from $I_s(\lambda)$ and $I_0(\lambda)$, that is, the UV light intensity after the passage of the hot flue gas with and without SO_2 seeding, respectively; N is the molecular number density of SO_2; and L is the total optical path length which was evaluated to be 0.488 m. The errors in the calculation of the absorption cross section of SO_2 mainly originated from the evaluation of the number density and the path length. The error of the SO_2 number density introduced from mass flow controllers was less than ±1% according to the specified accuracy. The decrease of SO_2 concentration and temperature at the edge of the hot flue gas (see Figure 2b) due to the entrainment of ambient air could influence the homogeneity and introduce errors to the spectrum, especially at the wavelengths where the absorption cross section was sensitive to the temperature.

In the present study, SO_2 was mixed in the unburnt premixed jet flow and introduced into the burner. The spectrally resolved absorbance of SO_2 in the hot flue gas was obtained as described in the previous investigation,[22] which was the natural logarithm of the ratio between the intensity of the UV light after the passage of the hot flue gas in cases with and without SO_2 seeding (see eq 1). The typical absorbance of SO_2 obtained in the hot flue gas is presented in Figure 3. The

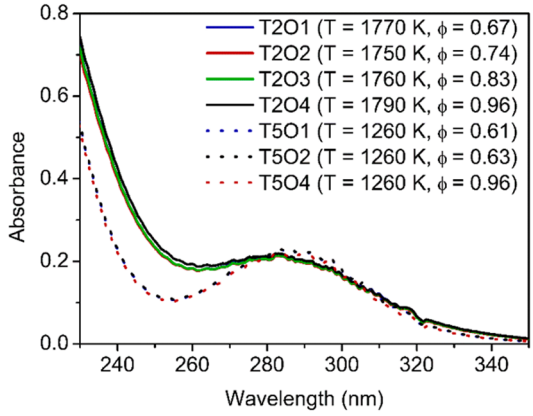

Figure 3. Absorbance of SO_2 with a constant number density in the hot flue gas provided by different lean flames at around 1750 K (T2O1−T2O4) and around 1260 K (T5O1−T5O4).

hot flue gas was provided by fuel-lean flames T2O1−T2O4 and T5O1−T2O4, with a variation in temperature and oxygen volume rate. The number density of SO_2 in the hot flue gas was kept constant at 6.2×10^{15} cm^{-3}, which was evaluated based on the concentration of SO_2 in the unburnt premixed gas. It was assumed that almost all the sulfur was in the form of SO_2 in the lean flames according to the chemical equilibrium calculation, where over 99% of sulfur was in the form of SO_2.[23] This assumption was supported by the phenomenon that the absorbance value was independent from the equivalence ratio for the cases which had the same temperature but varying equivalence ratios, as shown in Figure 3. With the known number density of SO_2 in the hot flue gas and the total path length, the UV absorption cross sections of SO_2 at certain

DOI: 10.1021/acs.analchem.9b02505
Anal. Chem. 2019, 91, 10849−10855

temperatures were calculated from corresponding absorbance using eq 1.

The UV absorption cross sections of SO_2 at temperatures from 1120 to 1950 K as the function of wavelength from 230 to 350 nm are presented in Figure 4, together with the

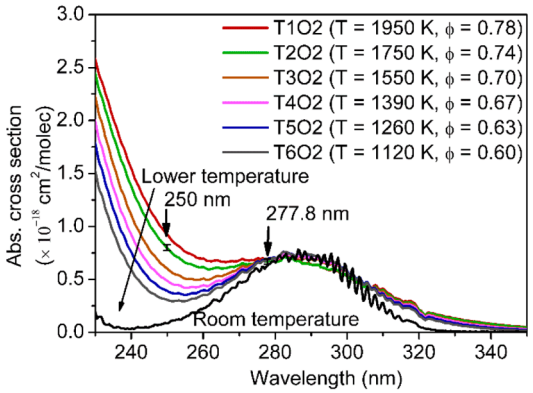

Figure 4. UV absorption cross sections of SO_2 at room temperature and the temperature varying from 1120 to 1950 K. Typical standard deviations from 10 independent measurements at 250 and 277.8 nm are marked in the spectral curve.

absorption cross sections at room temperature (296 K). All absorption spectra have a similar structure with a broad band absorption peak at the wavelength of around 290 nm, which was mainly attributed to the $\tilde{A}(^1A_2) \leftarrow \tilde{X}\ (^1A_1)$ transition forming the structured bands and the $\tilde{B}(^1B_1) \leftarrow \tilde{X}(^1A_1)$ transition forming the "continuous" absorption in the range 240−340 nm.[5] At room temperature, the absorption cross sections obtained here are very close to the ones reported by Vandaele et al.[5] and other references therein. As the temperature is increased over 1120 K, the line structures on the broad absorption band disappeared. The absorption cross sections increased with temperature, especially in the low wavelength region, for example, the wavelength below 260 nm. There is a strong absorption in the range 170−230 nm corresponding to the $\tilde{C}(^1B_2) \leftarrow \tilde{X}\ (^1A_1)$ transition.[5] At elevated temperature, this band becomes broader. Consequently, the absorption up to 266 nm is significantly increased compared to the room temperature case in Figure 4. For example, at 250 nm, the absorption cross section increases from $\sim 0.1 \times 10^{-18}$ to $\sim 0.9 \times 10^{-18}$ cm^2/molecule as the temperature rose from room temperature to 1950 K. However, around 280 nm, the changes were shown to be very small, especially around 277.8 nm; a constant absorption cross section, that is, 0.68×10^{-18} cm^2/molecule, was obtained. This phenomenon at elevated temperature was also observed by Grosch et al.,[7] Vattulainen et al.,[6] and Hippler et al.[13] The absorption cross section at 277.8 nm obtained in the present investigation is close to the one obtained by Grosch et al.[7] at 773 K and Vattulainen et al.[6] at 1073 K and 4 bar, with a value of $\sim 0.7 \times 10^{-18}$ and $\sim 0.8 \times 10^{-18}$ cm^2/molecule, respectively. It is much larger than the value 0.28×10^{-18} cm^2/molecule reported by Hippler et al.[13] at 1500 and 2000 K with shock-wave heating.

In addition, the cross sections at wavelengths of 250 and 277.8 nm with different temperatures are presented in Figure 5. It can be seen that the absorption cross section at 250 nm increased with temperature while the one at 277.8 nm has almost a constant value. The ratios of the cross section at 250

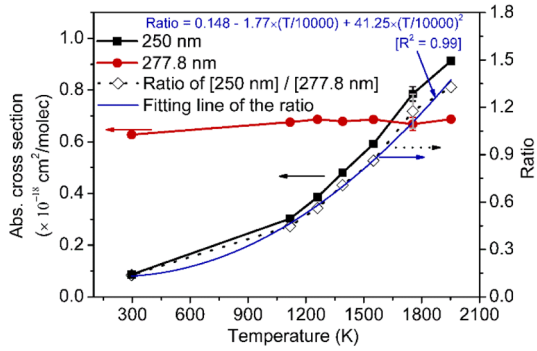

Figure 5. UV absorption cross sections of SO_2 at 250 and 277.8 nm with varying temperature, and the ratios between them with the corresponding parabolic fitting line.

nm to the cross section at 277.8 nm are shown in Figure 5. It can be well fitted by a parabolic curve. On the basis of the ratios, which are sensitive to the temperature, optical thermometry can be developed for in situ temperature measurement.

To have a concentration measurement of SO_2 without the effect of temperature, the absorption cross section at the wavelength of 277.8 nm was used for the concentration evaluation in the following studies. With use of this absorption cross section, the concentration of SO_2 in hot flue gas provided by the flame T2O2 (T = 1750 K, ϕ = 0.74) was measured as a different amount of SO_2 was mixed in the unburnt premixed gas. The results are shown in Figure 6 and standard deviations

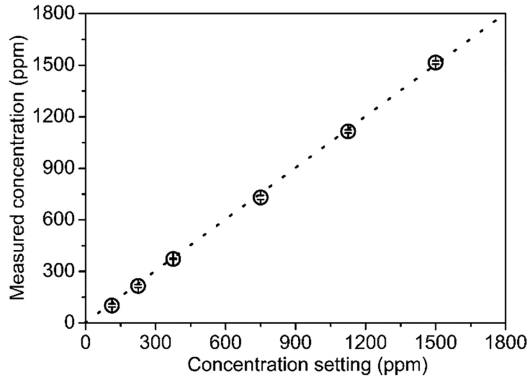

Figure 6. Concentration measurement with a different amount of SO_2 in the hot flue gas provided by the flame T2O2 (T = 1750 K, ϕ = 0.74).

observed in measurements were almost constant. The standard deviation from 10 independent measurements was analyzed to be around 10 ppm, where each measurement had an integrating time of 1 s. Hence, a conservatively estimated precision was obtained with a lower concentration of SO_2; for example, the relative uncertainty could be around 10% with 100 ppm SO_2.

As discussed above, the concentration of SO_2 in fuel-lean combustion environment can be well measured by the UV absorption technique. However, in fuel-rich environments, other sulfur species, such as H_2S, CS_2, OCS, and S_2, could be formed.[23] These species also have UV absorption in the same wavelength region as SO_2, which could influence the accuracy of SO_2 measurement. Hence, the measurement of SO_2 in fuel-rich flames was also investigated. The absorbance in the hot

DOI: 10.1021/acs.analchem.9b02505
Anal. Chem. 2019, 91, 10849−10855

flue gas provided by the fuel-rich flame T2O7 (T = 1750 K, ϕ = 1.32) with seeding of 1500 ppm SO_2 are presented in Figure 7. As the SO_2 was seeded into the rich flame conditions, similar

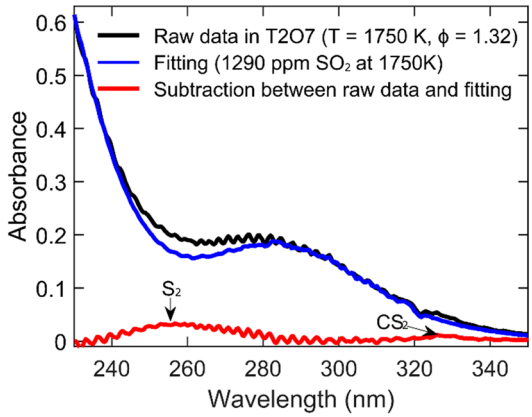

Figure 7. Absorption spectrum of SO_2 having a constant number density in the environments provided by the flames with different equivalence ratios, including the fuel-lean case, T2O2 (T = 1750 K, ϕ = 0.74), and fuel-rich case, T2O7 (T = 1750 K, ϕ = 1.32).

absorption curves were obtained. However, some extra absorption structures with multipeaks were observed, which indicates that some other sulfur species contributed to the absorption. At around 290 nm, the absorption cross section of H_2S (~5 × 10^{-20} cm^2/molecule), OCS (2 × 10^{-20} cm^2/molecule), and CS_2 (1 × 10^{-20} cm^2/molecule) at 773 K reported by Grosch et al.[24] and the absorption cross section of S_2 at 298 K reported by Sarka et al.[25] were significantly smaller than the one of SO_2 shown in Figure 4. The absorption at around 290 nm in Figure 7 was mostly attributed to SO_2. Hence, on the basis of the value at 290 nm, the absorbance in Figure 7 was fitted by the absorption cross-section spectrum of SO_2 at 1750 K (see Figure 4) with a concentration of 1290 ppm, which indicates that, as 1500 ppm SO_2 was seeded into the hot reductive environment, there was about 86% of SO_2 remaining. In a comparison of the raw data of the absorbance and the fitting curve to those from SO_2, some differences were observed, especially at around 260 nm. This was caused by the absorption of other sulfur species. The subtraction between the raw data and the fitting curve was conducted and is presented in Figure 7. According to the absorption cross-section spectra of H_2S, OCS, CS_2, and S_2, the absorption peak around 260 nm was attributed to S_2 and the one around 330 nm was attributed to CS_2. Therefore, with a proper fitting process, the measurement of SO_2 in the reductive environments with a known temperature are achievable. However, the accurate absorption cross section of H_2S, OCS, CS_2, and S_2 at high temperature are needed to give a more precise analysis.

Laser-Induced Fluorescence of SO_2 Excited by 266 nm Laser. The LIF of SO_2 excited by the 266 nm laser was applied in the concentration measurement of SO_2 in combustion atmospheres. First, the spectrum of the LIF emission of SO_2 in the hot flue gas were recorded by a spectrometer. In the measurement, the number density of SO_2 in the premixed unburnt gas was kept constant, and the hot flue gas had different temperatures, which was provided by different flames with varying equivalence ratios. The spectra are presented in Figure 8. All the spectra have a similar structure, except for the case obtained at room temperature.

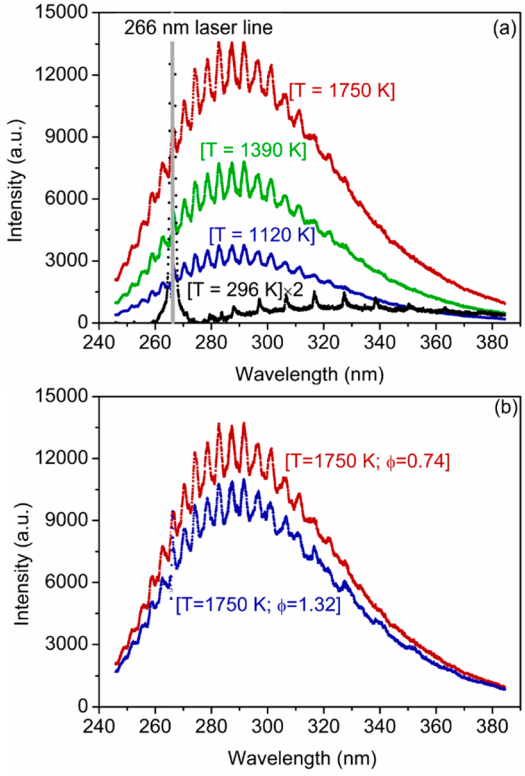

Figure 8. Spectra of the fluorescence emission of SO_2 excited by a 266 nm laser at different temperatures (a) and equivalence ratios (b).

The fluorescence could be released from the excited states, $\tilde{C}$ ($^1B_2$), $\tilde{B}$ ($^1B_1$), and $\tilde{A}$ ($^1A_2$), after the transition from the $\tilde{X}$($^1A_1$) state with the excitation of the 266 nm laser beam. At room temperature, excited at 266 nm, there is no absorption contributed from the $\tilde{C}$ ($^1B_2$) ←$\tilde{X}$($^1A_1$) band as shown in Figure 4. Hence, SO_2 molecules were mostly excited to the hybrid energy states, $\tilde{B}$ ($^1B_1$) and $\tilde{A}$ ($^1A_2$).[17] The broad band emission in the room temperature case in Figure 8 originated from the relaxation of SO_2 molecules to the ground state during the second time population process.[17] Moreover, the distinct vibrational structure with a line spacing of about 1050 cm^{-1} was observed with the relaxation of SO_2 molecules from the excited state after the second time population process. It has been investigated by Sick[18] that the spacing was almost 2 times that of the vibrational frequency, that is, 517 cm^{-1} of the asymmetrical stretching mode of the $\tilde{X}$ ($^1A_1$) state, which was caused by the selection rule (Δv = ±2, ±4, etc.) of an asymmetric vibration.[18,26] At elevated temperature, the absorption cross section at 266 nm had a significant increase because of the contribution from the $\tilde{C}$ ($^1B_2$) ← $\tilde{X}$ ($^1A_1$) transition. Hot SO_2 molecules were partially excited to the $\tilde{C}$ ($^1B_2$) state by the 266 nm photons and the red-shifted fluorescence was emitted. Considering that the fluorescence from the $\tilde{B}$ ($^1B_1$) state and the $\tilde{A}$ ($^1A_2$) state was weak,[14] the fluorescence from the $\tilde{C}$ ($^1B_2$) state dominated the signal at high temperature as shown in Figure 8. A stronger emission was obtained from SO_2 at a higher temperature. For the fluorescence, a vibrational structure with a line spacing of about 500 cm^{-1} was observed.

SO_2 LIF measurements at different equivalence ratios were performed and the results shown in Figure 8b indicate that the stoichiometric ratio has an influence on the LIF signal. It is mainly caused by the conversion of SO_2 into other sulfur

DOI: 10.1021/acs.analchem.9b02505
Anal. Chem. 2019, 91, 10849−10855

compounds, such as H_2S and S_2, in reduction environments.[23] However, in a comparison of the shapes of the fluorescence spectra from oxidative and reductive environments, there is no difference in the structure, which shows that there is no fluorescence emission originating from other sulfur compounds with the excitation of 266 nm laser.

For the spatially resolved imaging, an ICCD camera was employed to collect the fluorescence emission. A long pass filter, WG305, was used to suppress the scattering from the 266 nm laser. Figure 9a,b shows the intensity of the fluorescence signal as the function of the laser fluence and SO_2 concentration, respectively, in hot flue gas provided by the flame T2O2 (T = 1750 K, ϕ = 0.74). Good linear correlations were obtained. In Figure 9b, the relative standard deviation was found to be almost constant, around 1.3%. The absolute uncertainty was about 1.5 ppm for 100 ppm SO_2, while it was about 10 ppm using UV absorption spectroscopy. Moreover, with seeding 100 ppm SO_2, the signal-to-noise (S/N) ratio of the obtained fluorescence image was estimated to be around 100 (the obtained noise level was based on standard deviation of the background without signal), indicating that the detection limit of the LIF could be around several ppm. The LIF technique had a higher sensitivity in the measurement of SO_2 compared to the UV absorption spectroscopy technique.

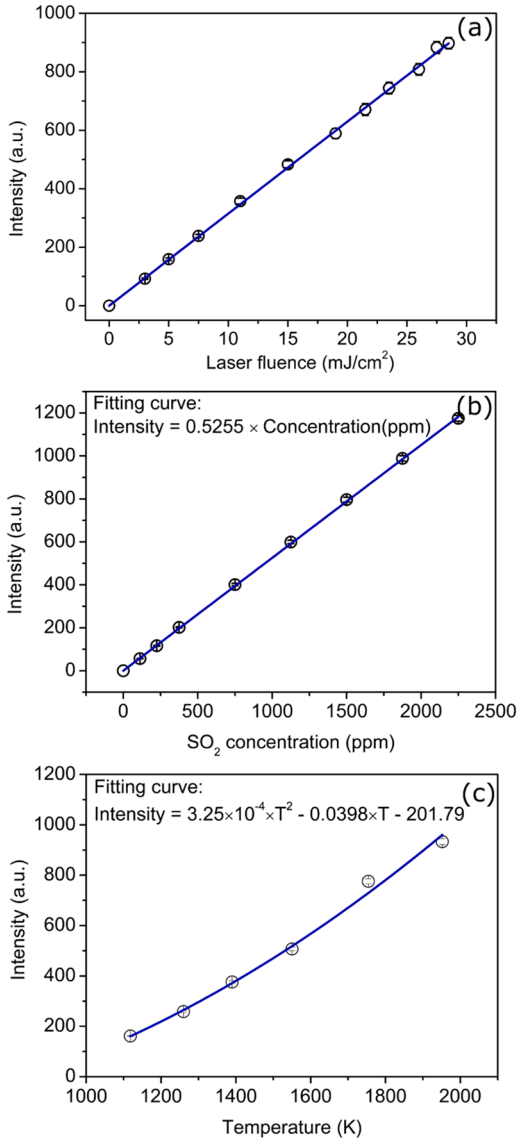

Figure 9. Intensity of the fluorescence emission signal of SO_2 as the function of the laser fluence (a), SO_2 concentration (b), and temperature (c).

On the basis of the linear relationship shown in Figure 9a, the SO_2 concentration could be easily evaluated through the obtained fluorescence emission signal. However, as illustrated in Figure 9c, besides the SO_2 concentration, the temperature could also influence the fluorescence emission signal. Measurements were conducted in the hot gas environments at temperatures from 1120 to 1950 K provided by flames T1O2−T6O2 with a constant number density of SO_2. An enhanced signal was obtained at a higher temperature, which corresponded to the increasing trend of the UV absorption cross section with the elevated temperature at 250 nm as shown in Figure 5. Different absorption at 266 nm affected the intensity of the fluorescence emission. The relationship between the emission intensity and the temperature was fitted by a parabolic equation (see Figure 9c).

With the calibration equations obtained in Figure 9b,c, the concentration of SO_2 in the combustion environments was measured using the LIF method with a known temperature. In the present study, a constant amount of SO_2 was introduced into the flames having different equivalence ratios, from fuel-lean to fuel-rich conditions. Then the concentration of SO_2 in the hot flue gas was obtained on the basis of its LIF signal. The results are presented in Figure 10. A constant concentration of SO_2 around 1500 ppm was obtained in the lean cases. For the cases with fuel-rich flames, the concentration of SO_2 was decreased, especially for the cases at the temperature of around 1800 K. The concentration reached around 1200 ppm as the equivalence ratio was over 1.2, which indicated that around 20% of SO_2 was converted to other sulfur species, which is close to the one we obtained through UV absorption spectroscopy. Compared to UV absorption spectroscopy, the LIF technique provided the concentration distribution of SO_2. It is more sensitive to the change in SO_2 concentration. However, to have quantitative results, calibration between the fluorescence signal and the SO_2 concentration and temperature was required. The uncertainty in both the temperature and laser power distribution might introduce errors into the final results.

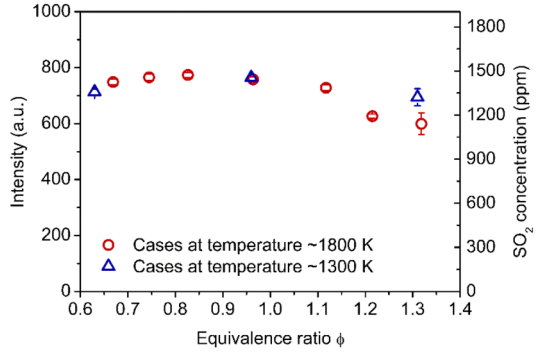

Figure 10. Laser-induced fluorescence signal and corresponding measured concentration of SO_2 in flames with different equivalence ratios and temperatures based on the fluorescence signal.

DOI: 10.1021/acs.analchem.9b02505
Anal. Chem. 2019, 91, 10849−10855

CONCLUSION

Broad band UV absorption spectroscopy and laser-induced fluorescence have been used for quantitative measurement of SO_2 in combustion environments. The UV absorption cross sections of SO_2 at temperatures ranging 1120−1950 K were obtained for the first time. It varied significantly with temperature as the wavelength was below 260 nm; however, around 277.8 nm, it almost remained constant at 0.68×10^{-18} cm^2/molecule, which can be used in the measurement of SO_2 concentration in combustion atmospheres with different temperatures. With use of the UV absorption spectroscopy setup, the measured results had a standard deviation of around 10 ppm. Moreover, the laser-induced fluorescence technique was adopted for the SO_2 measurement with a 266 nm laser. It is very sensitive in the SO_2 detection with a relative standard deviation of around 1.2%, that is, 2 ppm for the measurement of 100 ppm SO_2, which was more precise than the UV absorption spectroscopy. The disadvantage of this method is the requisite of calibration for a quantitative measurement. Consequently, it would be a good choice to combine the merits of the two methods for achieving highly sensitive and spatially resolved quantitative measurements of SO_2 in the combustion atmosphere.

AUTHOR INFORMATION

Corresponding Author

*E-mail: zhongshan.li@forbrf.lth.se (Z.L.).

ORCID

Zhongshan Li: 0000-0002-0447-2748

Notes

The authors declare no competing financial interest.

ACKNOWLEDGMENTS

The work was financially supported by the Swedish Energy Agency (GRECOP, No. 38913-2), the Knut & Alice Wallenberg Foundation (KAW 2015.0294, ALADIN), the Swedish Research Council (VR), and the European Research Council (ERC, No. 669466/TUCLA).

REFERENCES

(1) Ma, H.; Zhou, L.; Ma, S.; Wang, Z.; Cui, Z.; Zhang, W.; Li, J. *Energy Fuels* **2018**, *32*, 3958−3966.

(2) Christensen, K. A.; Stenholm, M.; Livbjerg, H. *J. Aerosol Sci.* **1998**, *29*, 421−444.

(3) Glarborg, P. *Proc. Combust. Inst.* **2007**, *31*, 77−98.

(4) Morelli, V.; Ziegler, C.; Fawibe, O. *Physician Assistant Clinics* **2019**, *4*, 185−201.

(5) Vandaele, A. C.; Hermans, C.; Fally, S. *J. Quant. Spectrosc. Radiat. Transfer* **2009**, *110*, 2115−2126.

(6) Vattulainen, J.; Wallenius, L.; Stenberg, J.; Hernberg, R.; Linna, V. *Appl. Spectrosc.* **1997**, *51*, 1311−1315.

(7) Grosch, H.; Fateev, A.; Nielsen, K. L.; Clausen, S. *J. Quant. Spectrosc. Radiat. Transfer* **2013**, *130*, 392−399.

(8) Mellqvist, J.; Rosén, A. *J. Quant. Spectrosc. Radiat. Transfer* **1996**, *56*, 187−208.

(9) Mellqvist, J.; Axelsson, H.; Rosén, A. *J. Quant. Spectrosc. Radiat. Transfer* **1996**, *56*, 225−240.

(10) Gao, Q.; Weng, W.; Li, B.; Aldén, M.; Li, Z. *Appl. Spectrosc.* **2018**, *72*, 1014−1020.

(11) Matsumi, Y.; Shigemori, H.; Takahashi, K. *Atmos. Environ.* **2005**, *39*, 3177−3185.

(12) Hieta, T.; Merimaa, M. *Appl. Phys. B: Lasers Opt.* **2014**, *117*, 847−854.

(13) Hippler, H.; Nahr, D.; Plach, H. J.; Troe, J. *J. Phys. Chem.* **1988**, *92*, 5503−5506.

(14) Rollins, A. W.; Thornberry, T. D.; Ciciora, S. J.; McLaughlin, R. J.; Watts, L. A.; Hanisco, T. F.; Baumann, E.; Giorgetta, F. R.; Bui, T. V.; Fahey, D. W.; Gao, R. S. *Atmos. Meas. Tech.* **2016**, *9*, 4601−4613.

(15) Bludský, O.; Nachtigall, P.; Hrušák, J.; Jensen, P. *Chem. Phys. Lett.* **2000**, *318*, 607−613.

(16) Fotakis, C.; Torre, A.; Donovan, R. J. *J. Photochem.* **1983**, *23*, 97−102.

(17) Zhang, G.; Zhang, L.; Jin, Y. *Spectrochim. Acta, Part A* **2010**, *77*, 141−145.

(18) Sick, V. *Appl. Phys. B: Lasers Opt.* **2002**, *74*, 461−463.

(19) Honza, R.; Ding, C.-P.; Dreizler, A.; Böhm, B. *Appl. Phys. B: Lasers Opt.* **2017**, *123*, 246.

(20) Borggren, J.; Weng, W.; Hosseinnia, A.; Bengtsson, P.-E.; Aldén, M.; Li, Z. *Appl. Phys. B: Lasers Opt.* **2017**, *123*, 278.

(21) Weng, W.; Borggren, J.; Li, B.; Aldén, M.; Li, Z. *Rev. Sci. Instrum.* **2017**, *88*, 045104.

(22) Weng, W.; Leffler, T.; Brackmann, C.; Aldén, M.; Li, Z. *Appl. Spectrosc.* **2018**, *72*, 1388−1395.

(23) Johnson, G. M.; Matthews, C. J.; Smith, M. Y.; Williams, D. J. *Combust. Flame* **1970**, *15*, 211−214.

(24) Grosch, H.; Fateev, A.; Clausen, S. *J. Quant. Spectrosc. Radiat. Transfer* **2015**, *154*, 28−34.

(25) Sarka, K.; Danielache, S. O.; Kondorskiy, A.; Nanbu, S. *Chem. Phys.* **2019**, *516*, 108−115.

(26) Herzberg, G. *Molecular Spectra and Molecular Structure: III. Electronic Spectra and Electronic Structure of Polyatomic Molecules*; Van Nostrand Reinhold Company: New York, 1953.

DOI: 10.1021/acs.analchem.9b02505
Anal. Chem. 2019, 91, 10849−10855